Dampening of Transverse Dispersion in the Halocline in Karst Limestone in the Northeastern Yucatan Peninsula

by Ronald K. Stoessell[a]

Abstract

A range of hydrodynamic dispersion coefficients was estimated for fracture-fluid and combined fracture and pore-fluid flow within the halocline of the limestone aquifer forming the surface of the northern Yucatan Peninsula. The coefficients are fit parameters in a model reproducing observed halocline profiles in a sinkhole and in a borehole near the northeastern coast. Fitted coefficients range from 10^{-7} to 10^{-4} cm^2/sec, of which molecular diffusion, without transverse (vertical) dispersion, can account for 10^{-7} to 10^{-5} cm^2/sec. The mechanical stability of the vertical density gradient in the halocline dampens transverse dispersion in pore fluids and in fracture fluids that are transitional between laminar and turbulent flow. The dampening is proportional to the ratio of the energy needed for the fluid to rise and displace a less dense fluid to the vertical component of the kinetic energy of the fluid. The ratio of these two energies is at a maximum during the initial stage of development of a halocline and decreases as the halocline widens.

Introduction

The northern Yucatan Peninsula (Figure 1) is a flat, low-lying, semitropical, Cenozoic limestone platform, having karst topography and lacking through-flowing rivers. Annual rainfall ranges from 0.5 m along the northern coast to 1.5 m along the eastern coast. The dimensions of the region are about 320 km east-west and 200 km north-south, with a maximum surface elevation of about 30 m (Back and Hanshaw, 1976). The peninsula is the site of rapid growth in population due to the developing tourist industry.

The surface limestone aquifer serves as the fresh-water aquifer for the peninsula. This aquifer contains a narrow fresh-water lens overlying saline water (sea water modified by water-rock interactions). The hydraulic head of the ground-water table at Chichen Itza, in the center of the peninsula (Figure 1) and 150 km from the eastern coast, was only 1.2 and 1.4 m above mean sea level in 1924 and 1966 (Back and Hanshaw, 1976). These hydraulic heads correspond, respectively, to 48 and 56 m thick fresh-water lenses in static, isostatic equilibrium with underlying sea water; although, the actual thickness will differ because the system is not static and perhaps not in isostatic equilibrium (Moore et al., 1992). The fresh-water lens thickness decreases towards the coast, becoming 30 and 18 m thick at Cenote Angelita and cenote Chemuyil, respectively, which are 12 and 6 km inland from the northeastern coast (Figure 1).

The coastal water-table elevation varies on the order of 0.1 to 0.2 m between rainy and nonrainy seasons; however, the total thickness of the coastal fresh-water lens does not vary significantly between seasons or on a yearly basis (Moore et al., 1992; Stoessell et al., 1993). The daily tidal range along the Caribbean coast is about 0.3 m and does not appear to affect the water-table elevation or the thickness of the fresh-water lens at distances greater than 2 km inland from the coast (Moore et al., 1992).

The limestone aquifer is a dual-porosity rock containing fractures and pores. In agreement with Wilson (1989), the author envisions fracture-fluid flow dominating over pore-fluid flow in the ground-water system. Fluids within the pores are likely to intersect fractures and join the fracture flow. Although some fracture fluids move out of the fractures into pores, the bulk of fracture fluids move within the fractures towards the coast. Fluids within the rock pores in the coastal region may have had significant fracture-flow portions of their travel path from the interior of the peninsula.

[a]Department of Geology and Geophysics, University of New Orleans, New Orleans, Louisiana 70148.

Received October 1993, revised April 1994, accepted October 1994.

Recently, Moore et al. (1992) reported measured average linear ground-water velocities in large fractures along the northeastern coast of the Yucatan Peninsula. The maximum measured fracture-flow velocities in fresh water increased from 1 cm/sec to 12 cm/sec along a 10 km coastward traverse, from Cenote Carwash to Cenote Tancah, along the Caribbean coast (Figure 1). This increase is presumed to result from the coastal wedging-out of the fresh-water lens as well as increased funneling of ground water from smaller fractures into larger fractures as the coast is approached (Moore et al., 1992). The fracture-fluid velocities are high values for ground-water flow; however, Worthington (1993) argues that the velocities within the fractures should be even higher.

Moore et al. (1992) also estimated average linear water velocities in pore fluids from point-dilution tests in an uncased borehole 2.6 km from the coast. These represented maximum velocity estimates and were 0.02 cm/sec in the fresh-water lens and 0.08 cm/sec in the underlying sea water, reflecting the nearby presence of a fracture. These two pore-fluid velocities are point measurements and are not necessarily representative of the pore-fluid environment.

The zone of brackish water separating the fresh water from the underlying saline water is called the halocline. The halocline thickness is surprisingly narrow, only 1 and 1.5 meters in width in Cenotes Angelita and Chemuyil, about 12 and 6 km, respectively, from the coast and 150 km from the interior of the peninsula (Figure 1). The narrowness of the haloclines suggests that diffusion, a slower process than transverse dispersion, is primarily responsible for their development. A less dense fluid (fresh water) overlying a more dense fluid (saline water) may act to dampen transverse dispersion.

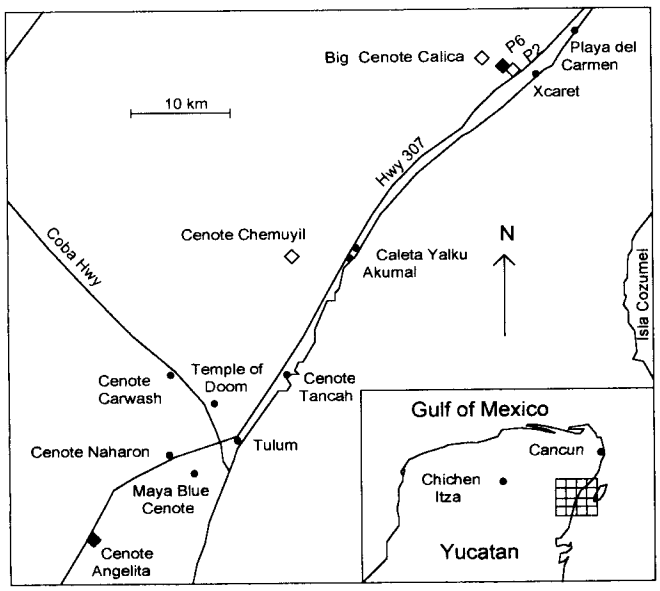

Fig. 1. Location map of the study area showing the sampling sites (marked with a diamond) for the depth-salinity profiles in Figure 3.

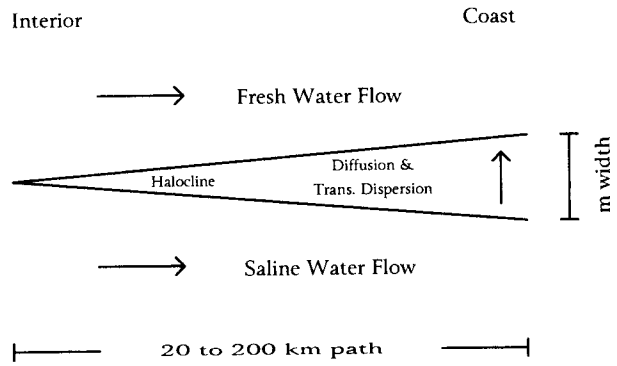

Fig. 2. Schematic model of the development of the halocline between underlying saline waters and overlying fresh waters.

Pollution problems are expected to increase in the fresh-water aquifer as the population increases. Pollutants injected in saline waters below the halocline may cross into the overlying fresh waters. In the absence of vertical advection, the rate of crossover will be controlled by transverse dispersion and molecular diffusion. For modeling purposes, the effects of these two processes are usually combined into the hydrodynamic dispersion coefficient, the parameter estimated in this study.

There are two purposes to this study. The first is to use the observed depth-salinity in a sinkhole and within a coastal borehole to estimate hydrodynamic dispersion coefficients. The second is to use these coefficients to assess the relative importance of diffusion versus transverse dispersion in developing the halocline and explain the apparent dampening of transverse dispersion.

Model Description and Assumptions

The simple molecular diffusion and transverse dispersion model is shown schematically in Figure 2. The fresh water and underlying saline water are assumed to flow horizontally towards the coast, from the interior of the peninsula, at equal velocities. Initially, the two ground-water zones are separated by a sharp interface. As the ground water flows coastward, molecular diffusion and transverse dispersion widen the interface into a brackish zone or halocline. Aquifer heterogeneity produces transverse dispersion during pore-fluid flow, and transitional turbulent flow produces transverse dispersion during fracture-fluid flow. Because transverse dispersion involves nonhorizontal fluid movement, a minor amount of vertical movement is included in the model in transverse dispersion.

Estimated path lengths of ground-water movement and a range of average linear flow velocities, constrained by field measurements, set limits on the time available for developing the brackish zone. The model is not intended to be used within a few km of the coast where wedging-out of the fresh-water lens has significantly increased fresh-water velocity, and tidal pumping causes vertical mixing.

The assumption that the underlying saline waters are not static and move towards the Caribbean Sea is consistent

with the saline waters, near the halocline, acting as the return arm of a sea-water convection cell (Cooper, 1959; Whitaker and Smart, 1990; Moore et al., 1992). The assumption of equal velocities of the underlying saline waters and the overlying fresh waters is an approximation suggested by the observed salinity-depth profiles at some of the field sites. If the saline waters are static or moving significantly more slowly than the fresh waters, diffusivity processes will result in a steeper depth-salinity gradient in the saline portion compared to the fresh-water portion of the halocline.

The depth-salinity gradient in the halocline can be modeled independently of horizontal flow if the saline waters and overlying ground water are moving at nearly equal velocities. Longitudinal dispersion can be neglected because of the large flux of solutes in the horizontal direction (Sudicky and Frind, 1981; 1982). The distribution of dissolved salts in a vertical column of water, at a given point along the horizontal ground-water flow path, is assumed to have resulted from molecular diffusion plus transverse dispersion. The model calculates the halocline width and vertical salinity gradient using estimated flow-path times.

Observed Salinity-Depth Profiles

Salinity-depth profiles, taken near the end of the dry season from 1990 to 1993, are shown in Figure 3 for several cenotes and for two coastal boreholes, located approximately 150 km from the center of the peninsula. The data are from the hydrology study by Moore et al. (1992), the water-quality studies by Stoessell et al. (1993) and Marcella (1994) and an unpublished 1992 study by Ron Stoessell. The salinities have been computed from conductivity measurements and calibrated with analytical measurements of the compositions of water samples. The salinity-depth profiles do not vary from year to year, indicating stable steady-state conditions.

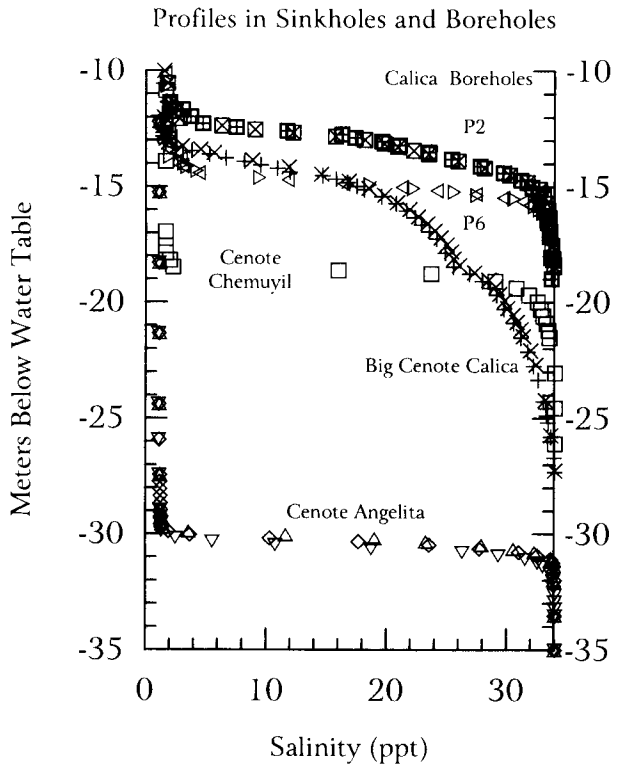

Fig. 3. Depth-salinity profiles at the following sites: Cenote Angelita (5/91, ▽; 4/92, △; 4/93, ◇), Cenote Chemuyil (4/92, □), Big Cenote Calica (4/92, ×; 4/93, +), Calica Borehole P2 (8/90, ⊞ ; 5/91, ⊠), and Calica Borehole P6 (8/90, ▷; 5/91, ◁).

The halocline profiles have similar shapes in Cenotes Angelita and Chemuyil and in Calica Boreholes P2 and P6. The distances from the coast for Cenotes Angelita and Chemuyil and Calica Boreholes P6 and P2 are about 12, 6, 3.6, and 2.6 km, respectively, and the halocline widths are approximately 1, 1.5, 2, and 3 m, respectively. The increased width in the halocline in the boreholes is generally due to the slower pore-fluid flow rates, providing more time for the haloclines to develop and perhaps to increased mixing in the less saline portion of the halocline as the fresh-water flow velocity increases towards the coast. Tidal effects would increase mixing in the more saline portion of the halocline and may be important in Borehole #2 which is the site closest to the coast.

At all sites, the average depth-salinity gradient is slightly steeper to much steeper in the more saline halocline zones, indicating the fresh-water flow velocity is greater than the saline-water flow velocity. In this study, the author has used the Cenote Angelita and Calica Borehole P6 sites where the gradients are **approximately the same** in both fresh-water and saline-water portions of the halocline. For these two locations, the resulting fit of the model to the data suggests the saline-water flow velocity approaches the fresh-water flow velocity in the vicinity of the halocline.

The data from Big Cenote Calica are included to show situations where simple diffusion and transverse dispersion cannot account for the salinity-depth distribution. Big Cenote Calica lies about 6 km inland from the coast (Figure 1). The discontinuity in the profile of the Big Cenote Calica is thought to reflect channeling of high salinity water in fractures within the halocline. The simple model used in this study does not fit the flow system at Big Cenote Calica.

Estimated Flow-Path Lengths, Average Flow Velocities and Flow-Path Times, and Turbulent Flow

The linear distance from the coastal region to the interior of the peninsula is about 150 km. Because the starting point for ground water reaching the northeastern coastal region is not known, a range in linear path lengths must be assumed. A range of path lengths of 20 to 200 km has been used in this study.

The measured average linear fracture-flow velocity 10 km from the coast was about 1 cm/sec which was the lower detection limit of the flow meter used by Moore et al. (1992). This value is greater than the average linear fracture-flow velocity from the interior, because it includes the effect of the coastal wedging-out of the fresh-water lens. For this study, I have assumed a range of average linear fracture-flow velocities from 0.05 to 0.5 cm/sec for ground water reaching Cenote Angelita. The range in time for ground water to

reach Cenote Angelita through fractures along pathways of 20 to 200 km is 0.1268 to 12.68 years.

As previously mentioned, less information is available on pore-fluid velocities. Complicating the problem is that a significant amount of the flow-path to a pore-fluid site probably occurred in fractures. For this study, the author has assumed the range of average linear flow velocities in the combined pore and fracture path leading to Calica Borehole P6 is an order of magnitude lower than in the fractures alone, or 0.005 to 0.05 cm/sec. The range of time for ground water to reach Calica Borehole P6 through the combined fracture and pore path along pathways of 20 to 200 km is 1.268 to 126.8 years.

The range in linear fracture-flow velocities of 0.05 to 0.5 cm/sec corresponds to 25° C Reynolds numbers for pure water of 55 to 555, respectively, assuming a fracture width of 1 cm. These values represent transition conditions between laminar and turbulent flow which occur at Reynolds numbers between 60 and 600 (Fetter, 1988). Within fractures the transverse dispersion results from turbulent flow.

Mathematical Model

The analytical solution to the diffusion plus transverse dispersion model for developing the halocline is given by Crank (1970, p. 12 and Fig. 2.3).

$$C_{(z,t)} - C_f = 0.5\,(C_s - C_f)\ \mathbf{erfc}[z/(4Dt)^{0.5}] \qquad (1)$$

where $C_{(z,t)}$ is the salinity at time t (sec) at a distance z (cm) from the original interface at time zero. The interface fluid maintains the average salinity of the two end-member fluids. C_s is 34 ppt, the initial salinity of the saline water. C_f is the initial salinity of the fresh water and is 1 ppt in Cenote Angelita and 2 ppt in Calica Borehole P6. D is the **fit parameter** in the model, the hydrodynamic dispersion coefficient which is the sum of the molecular diffusion coefficient plus the transverse dispersion coefficient. Selected values for **erfc**[z], the error-function complement are listed in Crank (1970, Table 2.1).

Results

The salinity data from Cenote Angelita and Calica Borehole P6 in Figure 3 have been replotted, respectively, in Figures 4 and 5 as a function of distance from the interface. The interface fluid has the average composition of the fresh water and saline water. The curves on Figures 4 and 5 have been computed from equation (1) for constant values, in cm units, of the equation parameter $(4Dt)^{0.5}$.

Curve b on Figure 4 provides the best fit to the Angelita data with an equation parameter of 40 cm. The parameter is used, with the previously estimated range in time for the ground water to reach Cenote Angelita of 0.1268 to 12.68 years, to calculate a range in D of 1×10^{-6} to 1×10^{-4} cm^2/sec. The estimated value of D is proportional to the linear ground-water velocity so that the maximum value corresponds to the maximum velocity of 0.5 cm/sec used in this study.

Curve b on Figure 5 provides the best fit to the Calica Borehole P6 data with an equation parameter of 65 cm. The parameter is used, with the previously estimated range in

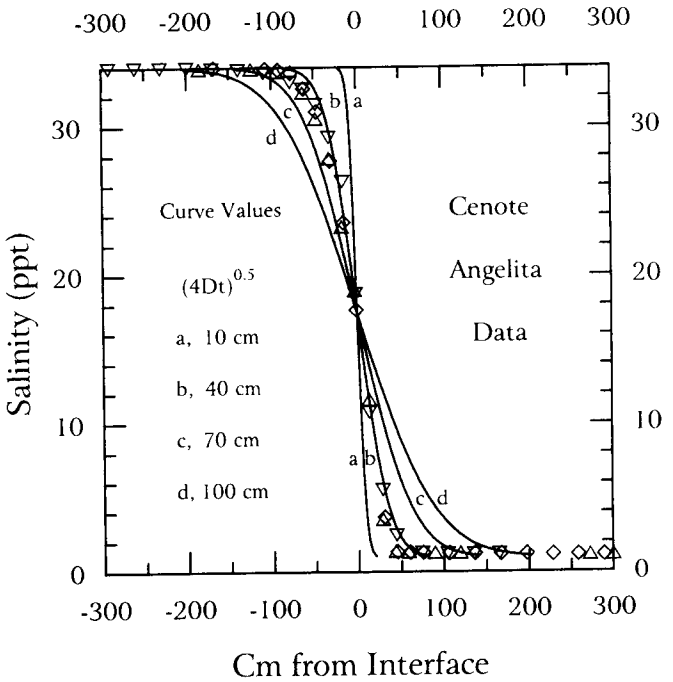

Fig. 4. Cenote Angelita salinities (5/91, ▽; 4/92, △; 4/93, ◇) plotted as a function of distance from the interface marking the average composition of fresh and saline waters. The solid curves were computed from equation (1) for constant values of $(4Dt)^{0.5}$.

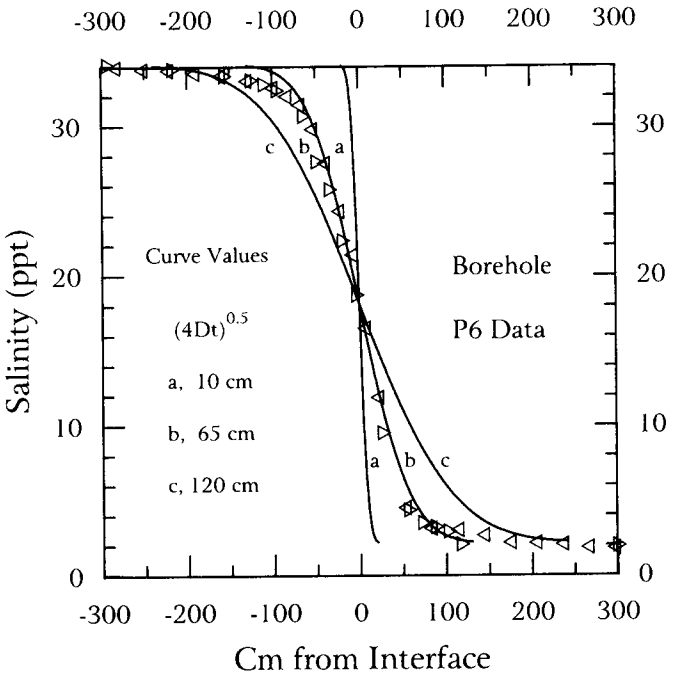

Fig. 5. Calica Borehole P6 salinities (8/90, ▷; 5/91, ◁) plotted as a function of distance from the interface marking the average composition of fresh and saline waters. The solid curves were computed from equation (1) for constant values of $(4Dt)^{0.5}$.

time for the ground water to reach Borehole P2 of 1.268 to 126.8 years, to calculate a range in D of 2.6×10^{-7} to 2.6×10^{-5} cm^2/sec.

The variability in the curves as a function of the equation parameter leads to an estimated error of less than 5 cm in picking the equation parameter which best fits the data. Taking this error into account increases the range in D to 2.3×10^{-7} to 1.3×10^{-4} cm^2/sec.

Discussion

The hydrodynamic dispersion coefficient can be split into the molecular diffusion coefficient D_m and the transverse dispersion coefficient D_t.

$$D = D_m + D_t \quad (2)$$

D_m in fluids has an expected value of about 1.5×10^{-5} cm^2/sec in an aqueous solution of 25° C which is the coefficient for NaCl diffusion in a 0.5 molar solution (Lerman, 1979). D_m in a porous or fractured medium has to be corrected for the solid matrix through which diffusion cannot occur. The correction involves multiplying the aqueous diffusion coefficient by the porosity fraction and dividing by the tortuosity squared (Stoessell, 1987). In the open-fracture pathway leading to Cenote Angelita, the porosity fraction is taken as one, the maximum possible value. In the combination fracture and pore system pathway leading to Calica Borehole P6, the average porosity fraction is taken as 0.5, an intermediate value between open fractures and the pores of the rock. The tortuosity, the ratio of the true path-length distance to the shortest distance, is assumed to range from 1 to 2 in the linear fracture system pathway leading to Cenote Angelita (Weidie, 1985) and between 2 and 3 in the combination fracture and pore system pathway leading to Calica Borehole P6. The overall tortuosity and porosity range corresponds to an overall range in D_m from 1.5×10^{-5} to 8.3×10^{-7} cm^2/sec. This range covers the lower portion of the estimated range in D, the hydrodynamic dispersion coefficient.

The maximum value of D_t, computed from equation (2) with the maximum estimate of D and the estimates of D_m, would be of the order of magnitude of 10^{-4} cm^2/sec. Hydrologists usually estimate D_t from the relation

$$D_t = a_t v \quad (3)$$

where a_t is the transverse dispersivity in cm, and v is the longitudinal (horizontal in this study) velocity.

Sanford and Konikow (1989a, 1989b) modeled Yucatan ground-water movement along the northeastern coast in a two-dimensional flow of a fluid of variable density through a heterogeneous, anisotropic, confined aquifer. Their model coupled equilibrium calcite dissolution with fluid flow to predict porosity development over tens of thousands of years. Sanford and Konikow used values of 50 cm for a_t, predicting steady-state vertical dimensions of the coastal haloclines between 20 and 40 m thick. These vertical dimensions are much larger than in the observed haloclines shown in Figure 3 and by Stoessell et al. (1989, Figure 3; 1993, Figure 2).

The maximum value of a_t, consistent with the maximum estimated value of D_t (for v equal to 0.5 cm/sec) is only 2×10^{-4} cm. This low value of a_t reflects the reduced effect of transverse dispersion, consistent with the observed haloclines having vertical dimensions of only a few meters.

The process of transverse dispersion in the halocline fluids requires packets of fluids to undergo vertical displacement. The path of the fluid packets is probably not vertical, but inclined at a small angle to the horizontal, resulting in a vertical displacement. However, the vertical density gradation in the halocline fluids is mechanically stable, with less dense fluids overlying more dense fluids. This mechanical stability dampens transverse dispersion, reducing the transverse dispersion coefficient.

The dampening effect on transverse dispersion in the halocline can be related to an energy ratio. Let N be the ratio of the displacement energy needed, for a unit volume of fluid to rise vertically a characteristic distance z and displace an equivalent volume of less dense fluid, to the vertical component of the kinetic energy possessed by the fluid.

$$N = g(p_f - p_{idf})\, z/[0.5p_f(v_h \tan \alpha)^2] \quad (4)$$

p_f and p_{idf} are the densities of the fluid and the less dense fluid respectively, g is the acceleration due to gravity, v_h is the horizontal fluid velocity, and α is the angle between the horizontal component of the flow velocity and the actual flow direction of the fluid packet undergoing dispersion. The term ($v_h \tan \alpha$) is the vertical component of the fluid velocity.

The larger the value of N, the greater the dampening effect on transverse dispersion. In this study N is at a maximum during the initial stage of formation of the halocline whan a sharp interface separates the overlying fresh water from the saline water (i.e., modified sea water). The maximum density difference would be between modified sea water and fresh water (with 1 ppt) with densities of about 1.025 and 1.001 g/cm^3, respectively. The angle α will be some small angle, assumed to be about 1 degree. For this situation with z equal to 1 micron (0.0001 cm), N ranges from 600,000 to 60 over the range of ground-water velocities used in this study, 0.005 cm/sec to 0.5 cm/sec. N is decreased by increasing the angle α and increased by increasing the vertical distance z. In a pore fluid, z would correspond to the grain diameter. Assuming α is 45 degrees and that z is one mm results in a range of N of 180,000 to 18 over the velocity range of 0.005 to 0.5 cm/sec.

As the halocline widens, the density difference decreases across z. At a density difference of 0.0001 g/cm^3, the range in N decreases from 2,500 to 0.25, assuming α is 1 degree and z is a micron. This decrease in N, as the halocline widens, reduces the dampening effect on dispersion, increasing the importance of transverse dispersion relative to molecular diffusion.

Acknowledgments

The author thanks Yolanda Moore for discussions on ground-water flow in the Yucatan and Dale Easley for discussions on diffusion and dispersion processes. The

author appreciates the time spent by three unknown journal reviewers who provided detailed comments that were used in revising the manuscript.

References

Back, W. and B. B. Hanshaw. 1976. Hydrogeochemistry of the northern Yucatan Peninsula, Mexico, with a section on Mayan water practices. In: Guide Book, Field Trip to Peninsula of Yucatan (revised), New Orleans Geological Society. pp. 211-243.

Cooper, H. H., Jr. 1959. A hypothesis concerning the dynamic balance of freshwater and saltwater in a coastal aquifer. Journal of Geophysical Research. v. 64, pp. 461-467.

Crank, J. 1970. The Mathematics of Diffusion. Oxford University Press, London. 347 pp.

Fetter, C. W. 1988. Applied Hydrogeology. Macmillan Publishing Company, New York, NY. 592 pp.

Lerman, A. 1979. Geochemical Processes Water and Sediment Environments. John Wiley and Sons, New York, NY 481 pp.

Marcella, L. M. 1994. Potential for dolomitization occurring in sea-water salinity fluids in the northeastern Yucatan Peninsula, Mexico (M.S. thesis). Univ. of New Orleans, New Orleans, LA. 55 pp.

Moore, Y. H., R. K. Stoessell, and D. H. Easley. 1992. Groundwater flow along the northeastern coast of the Yucatan Peninsula. Ground Water. v. 30, pp. 343-350.

Moore, Y. H., R. K. Stoessell, and D. H. Easley. 1993. Reply to Discussion of "Fresh-water/sea-water relationship within a ground-water flow system, northeastern coast of the Yucatan Peninsula." Ground Water. v. 31, pp. 321-322.

Sanford, W. E. and L. F. Konikow. 1989a. Porosity development in coastal carbonate aquifers. Geology. v. 17, pp. 249-252.

Sanford, W. E. and L. F. Konikow. 1989b. Simulation of calcite dissolution and porosity changes in saltwater mixing zones in coastal aquifers. Water Resources Research. v. 25, pp. 655-667.

Stoessell, R. K. 1987. Mass transport in sandstones around dissolving plagioclase grains. Geology. v. 15, pp. 295-298.

Stoessell, R. K., Y. H. Moore, and J. G. Coke. 1993. The occurrence and effect of sulfate reduction and sulfide oxidation on coastal limestone dissolution in Yucatan cenotes. Ground Water. v. 31, pp. 566-575.

Stoessell, R. K., W. C. Ward, B. H. Ford, and J. D. Schuffert. 1989. Water chemistry and $CaCO_3$ dissolution in the saline portion of an open-flow mixing zone, coastal Yucatan Peninsula, Mexico. Geological Society of America Bulletin. v. 101, pp. 159-169.

Sudicky, E. A. and E. O. Frind. 1981. Carbon 14 dating of groundwater in confined aquifers: Implications of aquitard diffusion. Water Resources Research. v. 17, pp. 1060-1064.

Sudicky, E. A. and E. O. Frind. 1982. Contaminant transportation in fractured porous media: Analytical solution for a system of parallel fractures. Water Resources Research. v. 18, pp. 1634-1642.

Weidie, A. E. 1985. Geology of the Yucatan Platform. In: Geology and Hydrogeology of the Yucatan and Quaternary Geology of Northeastern Yucatan Peninsula. New Orleans Geological Society, New Orleans, LA. 160 pp.

Whitaker, F. F. and P. L. Smart. 1990. Active circulation of saline ground waters in carbonate platforms: Evidence from the Great Bahama Bank. v. 18, pp. 20-203.

Wilson, W. L. 1989. Comment on "Porosity development in coastal carbonate aquifers." Geology. v. 18, pp. 200-203.

Worthington, S.R.H. 1993. Discussion of "Fresh-water/sea-water relationship within a ground-water flow system, northeastern coast of the Yucatan Peninsula." Ground Water. v. 31, p. 321.